Interaction of Antarctica with other regions at different spatial scales and deep layers

R. Kh. Greku[1] and D. R. Greku[2]

[1]Institute of Geological Sciences, National Academy of Sciences of Ukraine, 55b Gonchara St., Kiev, 01601, Ukraine (satmar@svitonline.com)
National Antarctic Scientific Center of Ukraine, 16 Tarasa Shevchenka Blvd, Kiev, 01601, Ukraine
[2]Satellite and MarineTtechnology Laboratory, Satmar-Australia, Great Western Pages Pty Ltd, Suite 206, 10 Norwest Central, Century Circuit, Baulkham Hills 2153 NSW, Australia (mailbag@greatwesternpages.com.au)

Abstract Structure, intraplate and interplate processes of the Antarctic region are interpreted down to a depth of 5300 km using a gravimetric tomography technique. The lateral and radial variability of four global-scale dense structures is displayed at depths of 5300 km and 2800 km and the relationship of these structures to Antarctica is outlined. It is then shown that the technique can be applied at more regional scales by providing interpretations of the gravity tomography in the areas of the Ross Sea / Scotia Plate and the Antarctic Peninsula at depth scales of a few kilometres down to>2000 km. Beneath the Scotia Plate, the thick transition layer above the 'Ross plume' is interpreted between depths of 620–1400 km. In the case of the Antarctic Peninsula, tomographic models display links between the Bransfield Basin and the Weddell Sea structures of the Powel basin and 'West Weddell Trench'.

Citation: Greku, R. Kh, and D. R. Greku (2007), Interaction of Antarctica with other regions at different spatial scales and deep layers, in Antarctica: A Keystone in a Changing World — Online Proceedings of the 10th ISAES X, edited by A.K. Cooper and C.R. Raymond et al., USGS Open-File Report 2007-1047, Extended Abstract 111, 4 p.

Introduction

The Earth's theories and tomographic data are important sources of information for the ISAES10 keystone problem "Antarctica in the Global Geodynamic System". Gravimetric tomography (Greku and Greku, 2006), lateral and vertical slices obtained through the geoid model, formed the basis for the research presented here. Seismic tomography data (Dziewonski and Woodhous, 1987; Bijwaard et al., 1998; Ritzwoller et al., 2001; Ishii and Tromp, 2001, 2004; Romanowicz, 2003a and 2003b) served as reference points. We started our study with the deepest layers to analyse the influence of geodynamic processes on the structure at shallower levels. A large spatial interaction between the Earth's layers as a result of relict tectonics is interpreted at the global scale. Regional processes are then considered for the Scotia lithosphere plate and for the Bransfield rift system.

Gravimetric tomography method and initial data

The gravimetric tomography technique included implementation of the following steps:

1. Determination of a relationship between the harmonic degree of the geoid height and the depth of the corresponding disturbing mass.
2. Determination of the harmonic density of anomalous disturbing mass relatively to the Preliminary Reference Earth Model (PREM).
3. 3D visualization of tomographic models of density inhomogeneities.

The spatial-scale of harmonics (half-wavelength), or lateral resolution, is 0.5°. Computing was carried out with an interval of 0.25°. Depth resolution between estimated earth layers is defined by an interval between depths which correspond to fixed harmonic's degrees. These intervals started at 0.5 km for depths of 1–20 km and increased greatly with increasing depth. In the figures below, blue colors indicate regions of less dense structures while yellow colors indicate more dense structures.

Structure and processes at the global scale

The distribution of global density inhomogeneities is shown on maps at depths of 5300 km and 2800 km in Figure 1. Four structures are located almost symmetrically within the Earth at the inner core surface at a depth of 5300 km. It is shown that the structures "1" and "2" have the most anomalous values in the epicenters (-1.4^{-5} and 1.37^{-5} g/cm^3 respectively), are of similar areas and have the largest gradients between them (100°E-120°E) on Earth. Locations of the structures coincide with geoid undulations (-102 m and 73 m) and the gradient zone is known as a region of catastrophic eruptions (e.g. Krakatau), earthquakes and tsunamis (e.g. 2004).

Structures "3" and "4" have lower values of density in their epicenters than structures "1" and "2". However, they are areally more extensive that structures "1" and "2"and, importantly, they extend south to Antarctica. Thus, the masses of structures "3" and "4" are an important contribution to the geodynamics of the Antarctic region at large depths and appear to 'block' extension of structures "1" and "2" to this region. This configuration is clearer in the polar projection of Figure 2, in which the convergence of four structures is shown. The intensity of the anomalies is reduced in the Antarctic region, and the gradients between the structures are smaller. A symmetrical influence of each of these

structures is interpreted as influencing the stable location of the Antarctic continent during the breakup of Gondwanaland, in contrast to other continents.

At a depth of 2800 km (Figure 1(b)), corresponding to the outer core, the Antarctic region is dominated by the structures "5" and "6", in the Ross Sea and to the south of Africa, respectively. These structures are discrete from the deeper structures "3" and "4". The boundary between structures "3" and "4" is located approximately orthogonal to the Antarctic coastline at 66°S; its longitudinal location varies from 100–137ºE, depending on the location of structure "5" at depth. Structure "5" (the 'Ross plume') is the most active in interaction with other dense (yellow) structures, in shallower layers also. It appears to have influenced the formation of the Australian–Antarctic Discordance within the ridge system of the Antarctic Plate boundary.

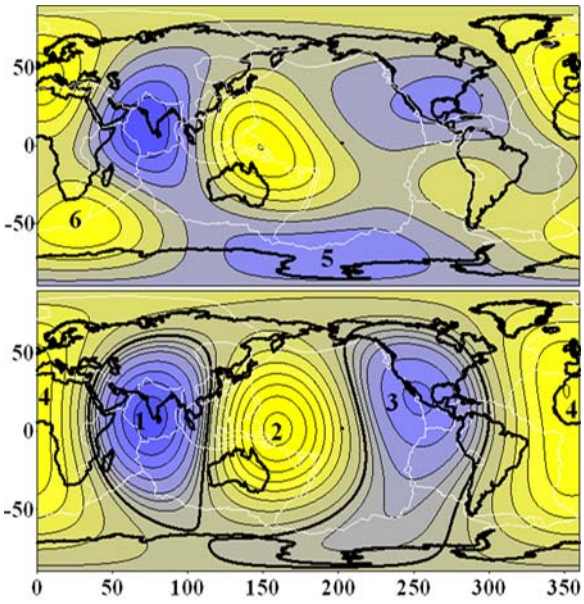

Figure 1. Distribution of dense (yellow) and thinning (blue) structures: (a) at the depth of 5300 km; and (b) at the depth of 2800 km (b). Spatial resolution is 0.5°. Structures: 1 – Indian Ocean, 2 – Pacific, 3 – North American, 4 – African, 5 – Ross plume, 6 – South African.

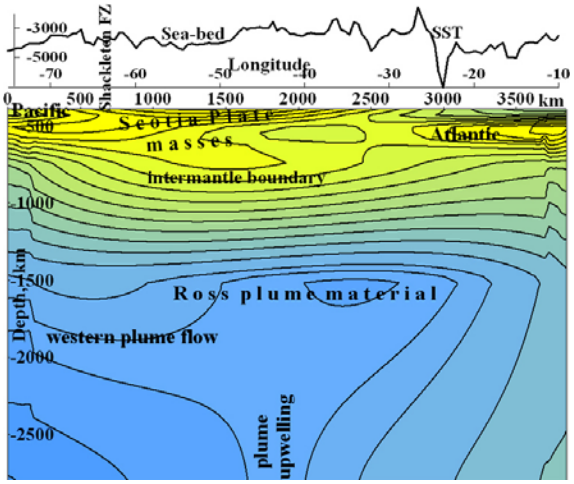

Figure 3. Distribution of dense heterogeneities along 58°S in the Scotia Sea (maximum anomalous values are -4^{-5} and 3.6^{-5}). Cross-section between depths of 390-2800 km. SST – South Sandwich Trench.

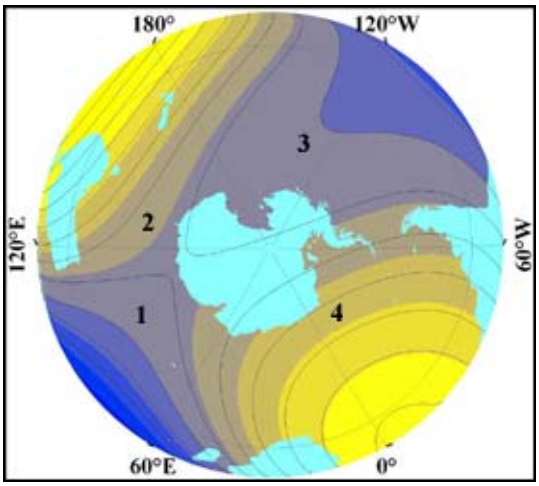

Figure 2. Antarctic region from Figure 1(a) in an orthographic polar projection. Note the convergence of structures "1" to "4" at the depth of 5300 km.

Regional structural features of the Scotia Plate

The Ross plume material is also interpreted to be present beneath the Scotia Sea in the cross-section along the central latitude of 58°S (Figure 3) and also along 43°W (not shown here). Mantle flow coming from the west (horizontal) and from ascending from below the Weddell Sea area are interpreted. The transition layer above the plume is interpreted at depths from 620–850 km down to 1400 km. The plume material eastward at a depth of approximately 1500 km to about 20–15°W. This observation supports the prediction of Leat (2002) that Pacific mantle flows eastwards beneath the Drake Passage. Figure 3 shows expansion of the Pacific mantle mass from the west (at depths of 400–480 km, distances of 0–600 km) and the Atlantic mantle mass from the east into a layer at depths of 500–610 km. The Scotia microplate is up to 310 km thick and it is moved by the Atlantic mantle masses significantly westward at depths of 200 km and deeper.

Links of the Bransfield Basin with the Weddell Sea

Much field research has been concentrated in the Bransfield Rift area, west of the Antarctic Peninsula (AP) (Janik et al., 2006; Canals et al., 1997; Galindo-Zaldivar et al., 2006; Berrocoso et al., 2006). We examined the structure of the region on both sides of the AP with several vertical cross-sections (Figure 4).

The extended section along 62.4°S between 70°W and 20°W down to a depth of 100 km is shown in Figure 5. It can be seen that the root part of the anomalous masses of AP is deflected eastwards under the influence of spreading of

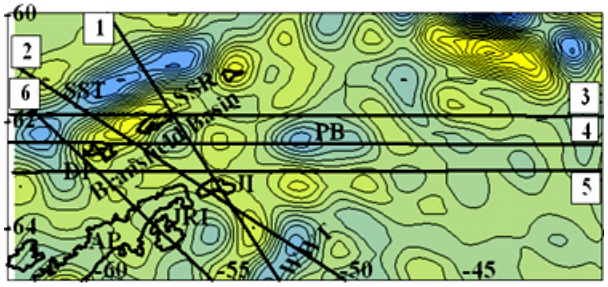

Figure 4. Map of the vertical sections across the Bransfield Basin. Background is a distribution of dense heterogeneities at the depth of 1 km. AP – Antarctic Peninsula, DI – Deception Island, JI – Joinville Island, JRI – James Ross Island, PB- Powel Basin, SSR – South Shetland Ridge, SST – South Shetland Trench, WWT – West Weddell Trench. 1-6 – numbers of cross-sections.

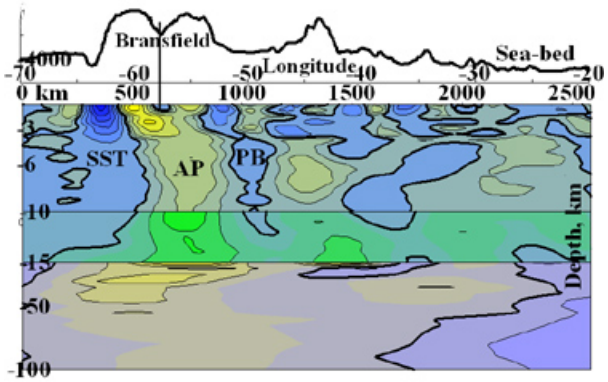

Figure 5. Cross-section of dense heterogeneities along 62.4°S down to a depth of 100 km (maximum anomalous values are -8^{-2} and 4^{-2}). For names see Figure 4.

the Pacific crust. This deflection is as much as 130 km at depths of 7–8 km. The Bransfield Rift channel is also displaced to the east.

The main sources of thinning masses in the Bransfield Basin (BB) come from the Weddell Sea (for example, the Powel Basin (PB) is such source interpreted in Figure 5). The connection between the Powel and Bransfield Basins is interpreted at depths of 1.8–2.5 km at a distance of 680–800 km along the profile. This westwards-ascending rift 'channel' is apparently blocked at about 710 km and at a depth of 2 km. There is another source of thinning material which is a structure located on the eastern margin of the AP at about 50°W. It is a structure located on the eastern margin of the AP at about 50°W. It appears to be a component of a subduction zone, similar to the South Shetland Trench (Galindo-Zaldivar et al., 2006). We refer to it as the 'West Weddell Trench' (WWT) in this paper. The WWT is not visible in the bathymetry but it is reflected in the geoid topography and especially in the differential geoid as a difference between the detailed altimetric geoid and the OSU91 geoid model (Schöne, 1997). These examples confirm the interpretation that the Bransfield rift channel plunges eastward (Canals et al., 1997 and Galindo-Zaldivar et al., 2006).

Agreement and difference between gravimetric and seismic tomographic results

As well as greatly improving our understanding of geodynamics, seismic tomographic data have provided information on the structure of the Earth at many depths and have lead to the development of new tectonic hypotheses. At the same time, it does not exclude the use of other methods which can be added to seismic tomography. In our study, we have looked for agreement and confirmation of our gravimetric tomography images with the available seismic tomography data. We have not always found such agreement. That is, a low radial resolution at large depth in the gravimetric tomography method does not allow us to identify low velocity anomalous heterogeneities on the core–mantle boundary. At the same time, there is a quite high lateral and radial resolution at shallow depths. Discrepancies between gravimetric and seismic tomographic results can be due to the techniques analyzing different physical properties of the earth, namely: the velocity of the seismic wave propagation and gravity data which then are inverted to provide density.

Consistent results between both tomographic methods are observed for many regions at the global scale from previous work (Ritzwoller et al., 2001, in which the best agreement is with the diffraction tomography; Shapiro and Ritzwoller, 2002; Ritzwoller et al., 2002). A similarity with relative perturbations in density at most depths is found in Ishii and Tromp (2001; in which the best agreement is with the whole-mantle density model when geoid coefficients are used) and Ishii and Tromp (2004). An appropriateness of the geoid data for the tomography is confirmed in Ricard et al. (1993) and Forte et al. (1994), where the observed geoid (gravitation potential) coefficients are used for evaluation and testing of the inverted density models predicted by the seismic models.

Summary

The structure and geodynamics of the interior of the Earth at large depths, which is interpreted to have influenced Gondwana breakup and to have formed the Antarctic lithosphere, are shown here with gravimetric tomography data. A thick layer of hot Ross plume material between depths of 620–1400 km is interpreted below the Scotia Plate along the central latitude of the region. Local tomographic models display links of the Bransfield Basin with the Weddell Sea structures of the Powel Basin and the West Weddell Trench. The errors of dense anomalies depends on errors of spherical function coefficients. These rms errors are of the order of 10^{-10}–10^{-8} for the EGM96 model that is much smaller than the computed anomalies.

Acknowledgements. The co-authors express thanks the co-editor and all reviewers for their significant work to improve this research paper. This work was supported by the National Antarctic Scientific Center of Ukraine.

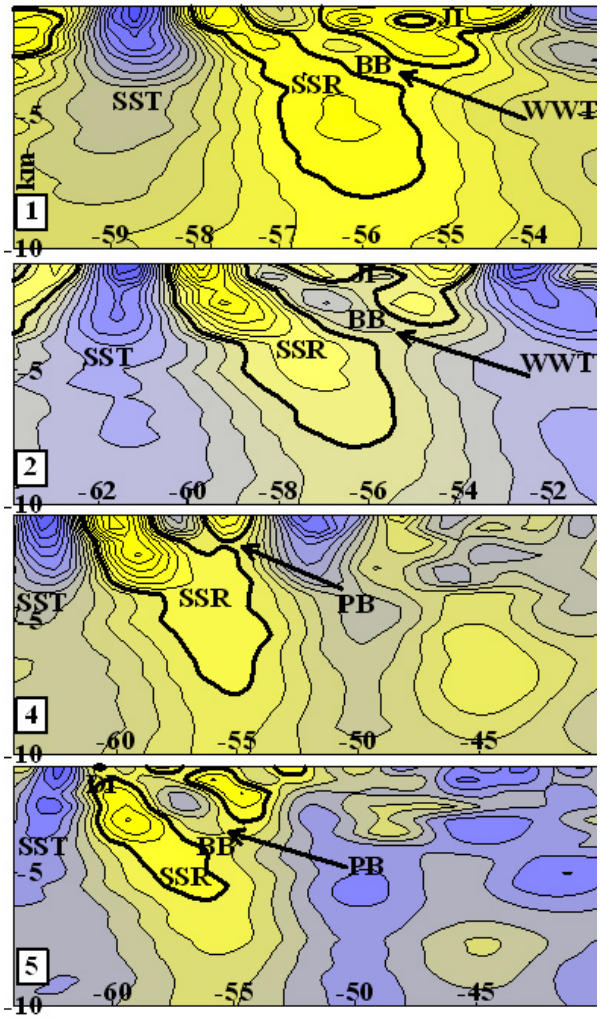

Figure 6. Four vertical sections of dense heterogeneities cross the BB, AP and Weddell Sea regions (maximum anomalous values are -6^{-2} and 6^{-2}). Arrows show channels of an entry of thinning masses from PB and WWT. Location of sections and abbreviations are in Figure 4.

References

Berrocoso, M., A. García-García, J. Martín-Dávila, M. Catalán-Morollón et al. (2006), Geodynamical studies on Deception Island: DECVOL and GEODETIC Ptojects, in: Antarctica - Contributions to Global Earth Sciences, Proceedings of the IX International Symposium of Antarctic Earth Sciences Potsdam, 2003, edited by D. K. Fütterer, D. Damaske, G. Kleinshmidt, H. Miller and F. Tessensohn, pp. 283-287, Springer, Berlin Heidelberg New York.

Bijwaard H., W. Spakman and E. R.Engdahl (1998), Closing the gap between regional and global travel time tomography, J. Geophys. Res., 103, B12, 30,055-30,078.

Canals, M., E. Gràcia, M. J. Prieto and L.M. Parson (1997), The very early stages of seafloor spreading: the Central Bransfield Basin, NW Antarctic Peninsula, The Antarctic Region: Geological Evolution and Processes, 669-673.

Dziewonski, A.M. and J. H. Woodhous (1987), Global images of the Earth's interior, Science, 236, 37-48.

Forte, A., R.L. Woodward and A.M. Dziewonski (1994), Joint inversion of seismic and geodynamic data for model of three-dimensional mantle heterogeneity, J. Geophys. Res., 99, B11, 21857-21877.

Galindo-Zaldívar, L., L. Gamboa, A. Maldonado, S. Nakao et al. (2006), Bransfield Basin tectonic evoluton, in: Antarctica - Contributions to Global Earth Sciences, Proceedings of the IX International Symposium of Antarctic Earth Sciences Potsdam, 2003, edited by D. K. Fütterer, D. Damaske, G. Kleinshmidt, H. Miller and F. Tessensohn, pp.243-248, Springer, Berlin Heidelberg New York.

Greku, R. Kh. and T. R. Greku (2006), Mantle and crustal structure of Antarctic along 170°W and 44°E meridians with the gravimetric tomography technique, in: Terra Antarctica Reports, No. 12, Proceedings of the Workshop on Frontiers and Opportunities in Antarctic Geosciences 2004, edited by C. Siddoway and C. A. Ricci, pp 145-154, Terra Antarctica Publication, Siena, Italy.

Ishii M. and J.Tromp (2001), Even-degree lateral variations in the Earth's mantle constrained by free oscillations and the free-air gravity anomaly, Geophys. J. Int., 145, 77–96.

Ishii M. and J.Tromp (2004), Constraining large-scale mantle heterogeneity using mantle and inner-core sensitive normal modes, Physics of the Earth and Planetary Interiors, 146, 113–124.

Janik, T., P. Środa, M. Grad and A. Guterch (2006), Moho depth along the Antarctic Peninsula and crustal structure across the Landward Projection of the Hero Fracture Zone, in: Antarctica - Contributions to Global Earth Sciences, Proceedings of the IX International Symposium of Antarctic Earth Sciences Potsdam, 2003, edited by D. K. Fütterer, D. Damaske, G. Kleinshmidt, H. Miller and F. Tessensohn, pp. 229-236, Springer, Berlin Heidelberg New York.

Leat Ph. (2002), Tracing mantle flow beneath the Scotia Sea, www.antarctica.ac.uk, British Antarctic Survey.

Ricard, Y., M. Ricards, C. Lithgow-Bertelloni and Y. Le Stunff (1993), A geodynamic model of the mantle heterogeneity, J. Geophys. Res., 98, B12, 21895-21909.

Ritzwoller, M. H., N. M. Shapiro, M. P. Barmin, and A. L. Levshin (2002), Global surface wave diffraction tomography, J. Geophys. Res., 107, B12, 2335, DOI:10.1029/2002JB001777.

Ritzwoller, M. H., N. M. Shapiro, A. L. Levshin and G. M. Leahy (2001), Crustal and upper mantle structure beneath Antarctica and surrounding oceans, J. Geophys. Res., 106, 12, 30645-30670.

Romanowicz, B. (2003a), Global mantle tomography: Progress Status in the Past 10 Years, Annu. Rev. Earth Planet. Sci., 31, 303–28, doi: 10.1146/annurev.earth.31.091602.113555.

Romanowicz, B. (2003b), 3D structure of the Earth's lower mantle, C. R. Geoscience. 335, 23–35.

Shapiro, N. M., and M. H. Ritzwoller (2002), Monte-Carlo inversion for a global shear-velocity model of the crust and upper mantle, Geophys. J. Int., 151, 88–105.

Schöne, T. (1997), The gravity field in the Weddell Sea, Antarctica, by radar altimetry from Geosat and ERS-1, Berichte zur Polarforschung, 220, Alfred Wegner-Inst fur Polar- und Meer-esforchung, Bremerhaven, Germany, pp. 145.